

Structural Defects in LB Films of Barium Salts of Fatty Acid
Based on X-Ray Analysis

Tisato KAJIYAMA,* Issei HANADA, Kenshiro SHUTO, and Yushi OISHI
Department of Applied Chemistry, Faculty of Engineering,
Kyushu University, Hakozaki, Higashi-ku, Fukuoka 812

Structural defects and crystalline dimensions in LB films prepared from barium salts of fatty acids with different alkyl chain length at various surface pressures were investigated on the basis of X-ray measurements. An increase in the alkyl chain length enhances the regularity in LB films. Not only the crystalline distortion in LB films but also the morphological heterogeneity of the monolayer caused the disorder along the longitudinal direction in LB films.

Langmuir-Blodgett (LB) films consist of a multilayered system of amphiphilic molecules. It has been considered that the LB films have the well-organized structure and, therefore, can be applied for various important functional characteristics, such as electric conductive¹⁾ and photo-electrical²⁾ properties. Recently several sorts of defects in the LB films have been discussed.³⁾ It is, therefore, indispensable to estimate the structural defects and crystalline dimensions in LB films and also, to investigate the procedure for constituting "defect-free" LB films for an interesting application of LB films to functional ultrathin organic films. In this study, the crystallite size and distortion along the parallel (lateral) and normal (longitudinal) directions to the layer plane of LB films were quantitatively evaluated on the basis of X-ray measurements. The effects of the preparation conditions and of the chemical structure of LB films on these structural parameters were also discussed.

In order to evaluate the structural parameters along the lateral direction in LB films, 200 monolayers of barium stearate ($2C_{18}Ba$), barium arachidate ($2C_{20}Ba$), and barium behenate ($2C_{22}Ba$) were deposited onto the polystyrene substrate at the surface pressures of 25, 30, and 35 $mN \cdot m^{-1}$, respectively, by the conventional LB method (transfer ratios:1). Further, the LB films of $2C_{18}Ba$ were prepared at 10, 15, and 40 $mN \cdot m^{-1}$ (transfer ratio:0.6, 0.8, and 1, respectively). Crystallite size L_{lat} and crystalline distortion D_{lat} along the lateral direction in LB films were estimated by a modified single line method⁴⁾ based on the Fourier analysis of wide angle X-ray diffraction (WAXD) profiles, because only one diffraction was detected on WAXD profiles of the LB films. Also, in order to evaluate the structural parameters along the longitudinal direction in LB films, 21 monolayers of barium palmitate ($2C_{16}Ba$), $2C_{18}Ba$, and $2C_{22}Ba$ were deposited onto cover glasses at 20, 30, and 35 $mN \cdot m^{-1}$, respectively, by the LB method (transfer

ratios:1). Also, the LB films of $2C_{18}Ba$ were obtained at 10, 15, and 40 $mN \cdot m^{-1}$ (transfer ratios:1). X-ray intensity at the small Bragg angle region was measured by a small angle X-ray scattering (SAXS) equipment with a Kratky U-slit camera.⁵⁾ Crystallite size L_{long} and crystalline distortion D_{long} along the longitudinal direction in LB films were calculated from the integrated width of the 001 SAXS peaks on the basis of the Hosemann paracrystal analysis.⁶⁾ The subphase temperature T_{sp} was 293 K and lower than the melting points of monolayers. Therefore, the LB films used in this study were in a crystalline state.⁷⁾ The melting behavior of monolayers and the aggregation state of crystalline or amorphous monolayer will be reported in detail elsewhere.⁸⁻⁹⁾

Table 1 shows L_{lat} and D_{lat} of the LB films of $2C_{18}Ba$, $2C_{20}Ba$, and $2C_{22}Ba$ prepared at the surface pressures at which each monolayer is morphologically homogeneous, that is, 25, 30, and 35 $mN \cdot m^{-1}$, respectively. L_{lat} calculated by the Scherrer's equation is also shown in Table 1. Moreover, L and Hosemann's disorder factor g of polyethylene (PE) single crystal mat estimated by the Hosemann's paracrystal analysis are shown in this table. The crystalline sizes estimated by a single line method are fairly comparable with those by the Scherrer's equation. Therefore, the single line method is applicable for estimating the crystalline structural parameters in LB films. The magnitude of D_{lat} decreased and that of L_{lat} increased with an increase of the alkyl chain length. This indicates that an increase of intermolecular aggregation force corresponding to an increase of the alkyl chain length enhances the regularity of crystalline phase in LB films. Crystalline regularity and crystallite size in all the LB films were smaller than those parameters of the PE single crystal.

Table 2 shows L_{long} , D_{long} , the observed bimolecular length d_{001} , and the calculated one based on the CPK molecular model (the most closed packing state of molecules) d_c of the $2C_{16}Ba$, $2C_{18}Ba$, and $2C_{22}Ba$ LB films prepared at the surface pressures at which each monolayer is morphologically homogeneous, that is, 20, 30, and 35 $mN \cdot m^{-1}$, respectively (d_c was calculated on the assumption that the diameter of a barium ion is 0.8 nm on the basis of the electron density distribution of the $2C_{18}Ba$ LB film¹⁰⁾). The difference $\Delta d = d_c - d_{001}$ decreased with increasing the alkyl chain length. It seems reasonable to consider that the conformation of alkyl chains tend to be a more extended one with an increase of the alkyl chain length because the value of d_c corresponds to the length of the most extended alkyl chain. The

Table 1. Crystallite size and distortion of LB films with different alkyl chain length along lateral direction

Amphiphiles	Distortion D_{lat} %	Crystallite size L_{lat}/nm	
		by single line method	by Scherrer's equation
$2C_{18}Ba$	4.1	7.7	10.8
$2C_{20}Ba$	3.9	9.0	12.7
$2C_{22}Ba$	3.7	11.5	14.5
Polyethylene (single crystal)	<2.0	30-50	

Table 2. Crystallite size and distortion of LB films with different alkyl chain length along longitudinal direction

Amphiphiles	Observed bimolecular length d_{001}	Calculated bimolecular length d_c	Δd	Crystallite size L_{long}	Distortion D_{long}
	nm	nm	nm	nm	%
$2C_{16}Ba$	4.46	5.07	0.61	46.8	3.7
$2C_{18}Ba$	5.06	5.57	0.51	56.8	2.8
$2C_{22}Ba$	6.15	6.57	0.42	59.4	2.4

magnitude of L_{long} almost corresponded to the thickness of 21 monolayers (bilayer spacing $\times 10.5$). The magnitude of D_{long} decreased with increasing the alkyl chain length. These results indicate that an increase of the intermolecular aggregation force causes more perfect crystalline regularity and larger crystalline continuity along the longitudinal direction in LB film. As schematically shown in Fig.1, the longitudinal regularity in LB films is always followed by the lateral one. Figure 1 shows the schematic representations of the perfect and disordered molecular aggregation states in LB films. The small closed

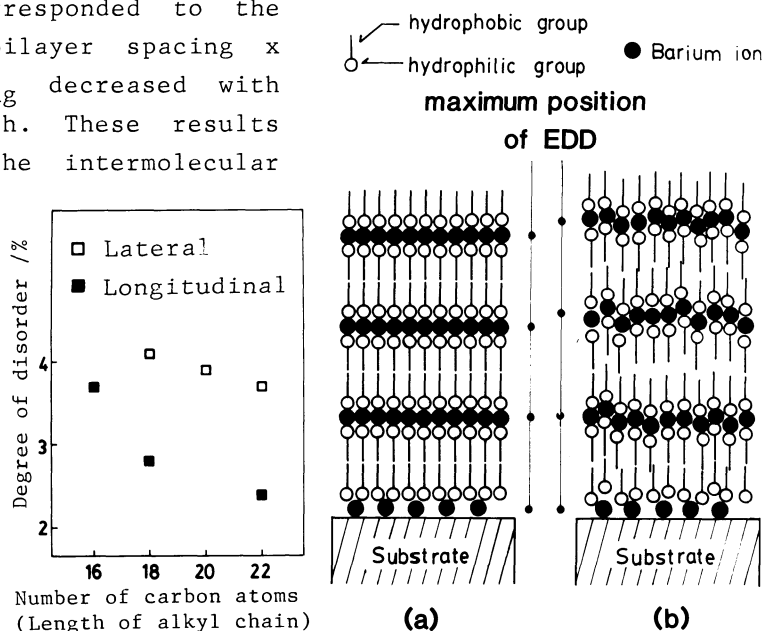


Fig.1. Schematic diagrams for crystalline defects in LB films at (a) perfect state; (b) disordered state.

circles represent the maximum positions of the electron density distribution (EDD) along the longitudinal direction in the LB films, in other words, the average repeating positions of the bilayer structure. The LB film of Fig.1(a) has the ordered structure not only along the lateral direction but also along the longitudinal one in LB film. On the other hand, Fig.1(b) shows a disorder alignment along the lateral direction in the LB film. A crystalline disorder along the lateral direction accompanies an irregular alignment of molecules along the longitudinal direction, as shown in the left-hand figure of Fig.1. Therefore, the molecular aggregation state of Fig.1(b) approaches that of 1(a) with an increase of the alkyl chain length of fatty acid salts.

Table 3 gives the magnitude of L_{lat} and D_{lat} in LB films of $2C_{18}Ba$ prepared at 15, 25, and 40 $\text{mN}\cdot\text{m}^{-1}$, respectively, as well as the morphological appearance of the monolayer.⁷⁾ The magnitude of D_{lat} increased and that of L_{lat} decreased with increasing the surface pressure. We reported⁷⁾ existences of crystalline monolayer domains at the surface pressure of 0 $\text{mN}\cdot\text{m}^{-1}$, of a homogeneous monodomain monolayer at 25 $\text{mN}\cdot\text{m}^{-1}$ and also, of a patchy morphology on the homogeneous flat monolayer due to the collapse of monolayer at 40 $\text{mN}\cdot\text{m}^{-1}$. The surface pressure dependence of crystalline monolayer morphology will be reported in detail elsewhere.⁹⁾ Thus, the apparent homogenizing of the monolayer surface with increasing the surface pressure up to 25 $\text{mN}\cdot\text{m}^{-1}$ does not influence the regularity of the crystalline phase in the LB film. Therefore, the monolayer after compression should be annealed or

Table 3. Crystallite size and distortion of $2C_{18}Ba$ LB films at different surface pressures along lateral direction

Surface pressure $\text{mN}\cdot\text{m}^{-1}$	Crystallite size L_{lat} nm	Distortion D_{lat} %	Morphology observation
15	8.1	4.0	island
25	7.7	4.1	homogeneous
40	6.7	4.3	collapse

recrystallized to reduce the amount of defects in LB film since the boundaries among the crystalline monolayer domains are one kind of crystalline defects.

Table 4 shows the magnitude of L_{long} , D_{long} , and the morphological appearance of $2C_{18}Ba$ monolayer transferred from the water surface at different surface pressures. The magnitude of D_{long} decreased with increasing the surface pressure up to $25 \text{ mN}\cdot\text{m}^{-1}$, and then, increased again at $40 \text{ mN}\cdot\text{m}^{-1}$. That is, the degree of the interlayer regularity (along the longitudinal direction in LB films) increases with increasing the morphological homogeneity of monolayers. The left part of Fig.2 shows the schematic representation of the heterogeneous monolayer morphology and the LB film prepared by depositing the heterogeneous monolayers. The right part of this figure shows the schematic representation of the homogeneous monolayer morphology and the LB film prepared by depositing the homogeneous monolayers. It seems apparent that the interlayer regularity in LB films decreases by depositing the heterogeneous monolayers onto the substrate.

In conclusion, to obtain the LB film with ordered molecular aggregation along the lateral and longitudinal directions, the monolayer of the amphiphiles with a larger intermolecular aggregation force has to be deposited onto the substrate at the surface pressure at which the monolayer surface is homogeneous.

References

- 1) T.Nakamura, M.Matsumoto, F.Takei, M.Tanaka, T.Sekiguchi, E.Manda, and Y.Kawabata, Chem.Lett., 1986, 709.
- 2) H.Kuhn, Pure Appl.Chem., 53, 2105(1981).
- 3) P.Lesieur, A.Barraud, and M.Vandevyver, Thin Solid Films, 152, 155(1987).
- 4) D.Hofmann and E.Walenta, Polymer, 28, 1271(1987)
- 5) "Small Angle X-Ray Scattering," ed by O.Glatte and O.Kratky, Chap.3, Academic Press, London(1982); Y.Sasanuma, Y.Kitano, and A.Ishitani, Polym.Prepr.Jpn., 35, 3592(1986).
- 6) "Direct Analysis of Diffraction by Matter," ed by R.Hosemann and S.N.Baguchi, North Holland, Amsterdam(1962).
- 7) T.Kajiyama, K.Umemura, M.Uchida, and Y.Oishi, Polym.Prepr.Jpn., 36, 3191(1987).
- 8) T.Kajiyama, N.Morotomi, M.Uchida, and Y.Oishi, submitted to Chem.Lett.
- 9) T.Kajiyama, Y.Tanimoto, M.Uchida, Y.Oishi, and R.Takei, submitted to Chem.Lett.
- 10) W.Lesslauer and J.K.Blasie, Biophys.J., 12, 175(1972).

Table 4. Crystallite size and distortion of $2C_{18}Ba$ LB films at different surface pressures along longitudinal direction

Surface pressure	Crystallite size L_{long}	Distortion D_{long}	Morphology observation
$\text{mN}\cdot\text{m}^{-1}$	nm	%	
10	47.6	4.3	island
15	44.6	3.3	island
25	56.8	2.8	homogeneous
40	49.9	3.1	collapse

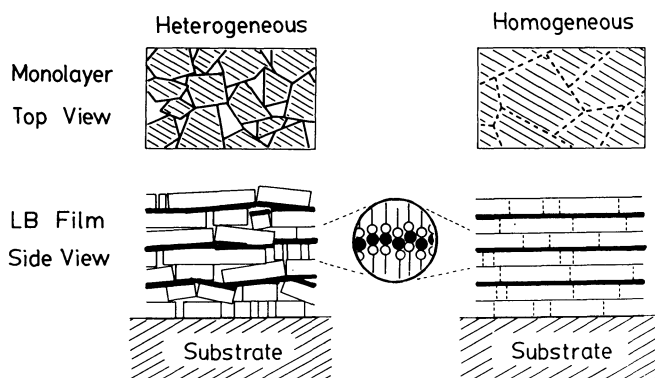


Fig.2. Layer structure in LB film deposited of monolayers with heterogeneous and homogeneous aggregation states.

(Received September 20, 1988)